Transition Modes in Adiabatic Spiral Vortex Flow in narrow and wide annular Gaps

C. C. Wan† and J. E. R. Coney‡

The stability of flow in a concentric annulus formed by rotating cylinders is well understood, but there is little information concerning the transitions which occur after the onset of spiral vortex flow. For both the narrow and wide gap cases ($N = 0{\cdot}8$ and $N = 0{\cdot}955$), it has been shown that the initial spiral flow breaks down from a quasiperiodic to a chaotic mode. Three axial Reynolds numbers were studied, viz., $Re_a = 500$, 1500, 2500. The introduction of digital techniques provided qualitative and quantitative information regarding the flow behaviour. The effects reported for $Re_a > 0$ and recent results of other workers for $Re_a = 0$ have been compared. The phenomenon of re-emergent flows has been observed at very high Taylor numbers and high axial Reynolds numbers.

NOTATION

$A_x(t)$	normalized autocorrelation function
ADC	analogue to digital converter
b	annular gap $(R_2 - R_1)$
d_e	equivalent diameter, $2(R_2 - R_1)$
f	frequency
f_c	frequency of inner cylinder
f_N	Nyquist frequency
i	index for the time signal $x(t)$
j	index denoting a complex number
k	length of integer record
L	length of integer record
M	number of samples
N	annular radius ratio (R_1/R_2)
$P_x(f)$	power spectral density function
R_1	radius of inner cylinder
R_2	radius of outer cylinder
Re_a	axial Reynolds number $(U_m d_e/\nu)$
t	time
Ta	Taylor number $\left(\frac{\Omega_1^2 R_1 b^3}{\nu^2}\right)\cdots$ narrow gap; $\left(\frac{2\Omega_1^2 R_1^2 b^3}{(R_1+R_2)\nu^2}\right)\cdots$ wide gap
Ta_c	critical Taylor number
U_m	mean axial velocity
$\bar{U}$	mean effective velocity (vector sum of axial and rotational velocity components)
u'	r.m.s. velocity fluctuations
V	mean voltage
v	voltage fluctuations
$x(t)$	a continuous time signal
$X(\omega)$	Fourier integral
$x(i)$	sequence of complex numbers which are functions of $x(t)$
$X(k)$	discrete representation of $X(\omega)$
$y(i\,\Delta t)$	discrete equivalent of time series $y(t)$
Ω_1	annular velocity of inner cylinder (rad/s)
Δt	sample time interval
ν	kinematic viscosity of fluid (m^2/s)
ω	frequency $(2\pi f)$

Received 4 February 1980 and accepted for publication on 25 April 1980

† Research Student | Department of Mechanical Engineering,
‡ Lecturer | University of Leeds, Leeds LS2 9JT.

1 INTRODUCTION

The early work by Taylor (**1**) on the problem of flow stability between concentric rotating cylinders has led to extensive investigations, both experimental and theoretical. With the addition of an axial pressure gradient, this problem increases in complexity, as the vortex flow adopts a spiral form. The early experiments of Snyder (**2**) and Schwarz *et al.* (**3**) showed that the spiral mode occurs at an axial Reynolds number, Re_a, of about 40. At $Re_a = 200$, the cells begin to develop into sinusoidal azimuthal waves, marking the beginning of the 'wavy' modes. Also, Coles (**4**) performed an excellent visual study of the evolution of these modes for $Re_a = 0$. However, because of the limitations of visual methods, these workers were confined to low values of Re_a. Theoretical stability predictions based on an infinite cylinder length and on the narrow gap approximation ($N \to 1$) by Chandrasekar (**5**), DiPrima (**6**), and Datta (**7**), showed that an axial flow component stabilizes the flow between rotating cylinders. These theoretical predictions agree well with the experiments of Donnelly and Fultz (**8**), Schwarz *et al.* (**3**), and Snyder (**2**). Using the modified Orr-Sommerfield equation, Hughes and Reid (**9**) extended theoretical investigations into higher values of Re_a. For $Re_a \approx 1000$, good agreement was found between their theory and the wide gap experiments of Kaye and Elgar (**10**), but there was substantial disagreement for higher values of Re_a. Hasoon and Martin (**11**), using the Galerkin method, computed values of the critical Taylor number, Ta_c, for $0{\cdot}9 \geqslant N \geqslant 0{\cdot}1$ at $Re_a \leqslant 2000$. These predictions were confirmed by the experiments of Gravas and Martin (**12**). All these theories were based on the assumption of axisymmetric disturbances, and such linear analyses were insufficient to predict instabilities at higher axial flows. However, Hughes and Reid (**9**) suggested a nonlinear theoretical approach based on non-axisymmetric disturbances.

0142/727X/80/0900-0131$02.00

In their investigations into higher Taylor and axial Reynolds numbers, Kaye and Elgar (**10**) and Astill (**13**) found, by means of hot wire anemometry techniques, that spiral vortex flow may be demarcated into four distinct flow regimes, viz., laminar, laminar plus vortices, turbulent, and turbulent plus vortices.

Using hot wire anemometry, experiments may be extended to higher flow ranges, provided adequate analogue recording instruments are available for quantitative analysis of the incoming signals. Fortunately, the limitations of conventional analogue instruments in terms of response to low frequency signals and resolution have been overcome by the advent of digital computers and analogue to digital converters (ADC), during the last two decades.

Gibson (**14**) improvised digital techniques for the recording and processing of laminar and turbulent flow data. He showed that the digital computer can perform most complicated analogue operations with comparable accuracy. Swinney and Gollub (**15**) reviewed the use of recent digital techniques for the measurement of instabilities in nonlinear systems, including rotational flow. They concluded that complex flow transitions, such as the quasiperiodic and chaotic stages, may be determined using laboratory computers and advanced signal processing techniques.

A qualitative study of flow instability in Taylor vortex flow ($Re_a = 0$) was carried out by Fenstermacher *et al.* (**16**), using laser doppler and digital techniques; the results of this investigation will be discussed in Section 4. The present work may be regarded as an extension of this research.

2 APPARATUS

The apparatus used was described in detail by Simmers and Coney (**17**). Basically, it consisted of a vertical concentric annular gap, having a rotating inner cylinder and a stationary outer cylinder with an axial length of 1820 mm. The outer cylinder was of radius 69·85 mm. Two interchangeable Tufnol inner cylinders of radius 66·4 mm and 55·9 mm were used to provide the narrow gap and wide gap configurations, respectively. The working fluid was air, which flowed down the annulus. Measurements were made at a distance of 1482 mm from the inlet, which was well within the region of fully developed flow, as determined by Simmers and Coney (**18**). Values of axial Reynolds number were determined by means of orifice plates, calibrated in accordance with BS1042.

Velocity measurements were taken using a DISA 55P71 dual wire probe in conjunction with a DISA anemometer unit. The apparatus was then interfaced to an analogue to digital converter (ADC), linked to the main computer. The continuous hot wire signals were sampled and converted into point voltage values to be reconstructed in the computer. The mean voltage, $V(t)$, was connected to one channel of the ADC, while the voltage fluctuations were low-pass filtered to remove the mean d.c. component and any high frequency noise. The resultant signal was then amplified and sent down a second ADC channel. All readings were taken at midgap position and the wires were orientated for maximum sensitivity. For the determination of fluid properties and

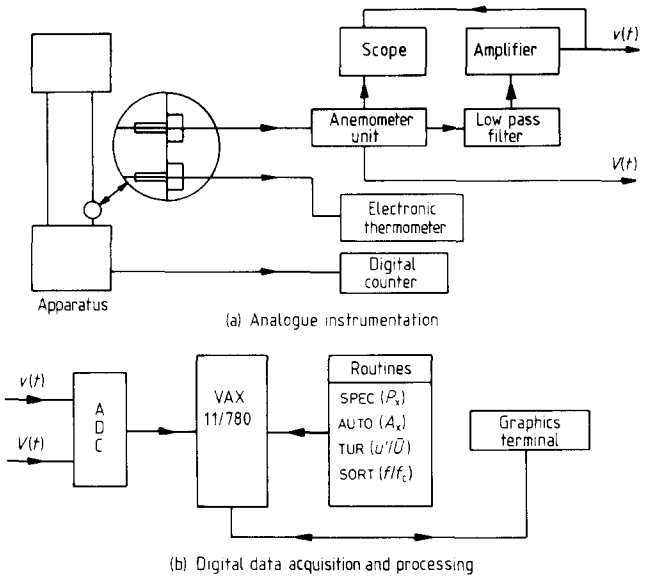

Fig. 1. Schematic representation of analogue and digital equipment

hence dimensionless groups, temperature measurements were made using a chromel-alumel thermocouple placed immediately downstream of the probe. The temperature was recorded by a Comark electronic thermometer to an accuracy of $\pm 0{\cdot}1°C$. The inner cylinder rotational speed was measured by means of a digital counter which recorded magnetic pulses from a pickup mounted near the base of the cylinder, its accuracy varying from 2 per cent at low speeds to 5 per cent at high speeds. Figure 1 is a schematic representation of the analogue and digital equipment.

3 PROCEDURE

3.1 Digital Techniques

Data records sampled and digitized by the ADC were analysed using a 32-bit VAX 11/780 computer. Sample record lengths (L) consisted of 33 seconds of recording time giving 16384 samples. The sample interval (Δt) chosen was 2 ms. It should be noted that vortex motion is primarily a low frequency velocity field having a range of 0·1 Hz to 20 Hz, depending on the axial flow component. The use of a mobile graphics terminal (Tektronix 4006-1) permitted the recording and analysis of the raw signals at the apparatus.

3.1.1 *Sources of errors* The main sources of error in digital data acquisition were noise contamination, clipping, and aliasing. Amplifying the signal before transmission to the ADC reduces the external noise pick-up by a signal : noise ratio greater than 40 dB. Clipping occurs when the mean d.c. component has not been sufficiently removed and the level of the signal exceeds the dynamic range of the ADC, viz., $\pm$ 10 volts; this leads to errors in computing the higher order derivatives of the signal. Also, corrections must be allowed for within the data acquisition program to correct any over-ranges or under-ranges encountered, provided that Δt is small enough to detect a large jump in the sampled value.

The problem of aliasing, described by Otnes and

Enochson (**19**), is present in all digital analyses of the present kind and results from the incorrect choice of sampling rate, causing the 'aliases' of higher frequencies in the power spectrum. According to Hancock (**20**) this may be avoided by choosing Δt such that it is twice the reciprocal of the Nyquist frequency (f_N). As a precaution, not only was this done, but also a sine wave generator, set to the appropriate frequency range, was connected, and other values of Δt were used to determine the best resolution for the length of samples to be recorded.

3.2 Data Analysis

Owing to the quantity, the data were stored on magnetic tape after a day's run. The software routines included the following analyses:

3.2.1 *Power spectrum* The power spectral density function $P_x(f)$ was computed by the fast Fourier transform algorithm.

The Fourier integral can be defined as:

$$X(\omega) = \frac{1}{2\pi}\int_{-\infty}^{\infty} x(t)\, e^{-j\omega t}\, dt \qquad (1)$$

and the algorithm computes the discrete form as:

$$X(k) = \frac{1}{M}\sum_{i=0}^{i=M-1} x(i) \exp\left(-j\frac{2\pi ik}{M}\right) \qquad (2)$$

The function $P_x(f)$ is derived from the complex Fourier coefficients resulting from the computation.

A serious problem in the spectral analysis is leakage, which arises because of the presence of harmonic components in the signal, the frequencies of which are not integer factors of the analysis interval. This causes the signal power to be distributed or 'leaked' over a range of frequencies. For example, if the signal has frequency f, the Fourier analysis will have a sharp peak at that frequency and, in addition, a series of peaks appears over the neighbouring frequencies. Earlier analyses, consisting of 1024 samples without any smoothing, resulted in this occurring in the spectrum of a sine wave. With the introduction of the 32-bit computer, a larger number of samples could be recorded and this problem was eliminated. In view of the length of the data records, partitioning into shorter lengths was resorted to, without loss of resolution. The theoretical resolution may be obtained by computing the spectrum for a generated sine wave and its full width at half-maximum of the spectral peak (after Otnes and Enochson (**19**)). With a record of $L = 8192$ samples, using a Hanning data window, a resolution of 0·008 per cent of the Nyquist frequency was obtained. The computed spectrum for each partitioned segment was then averaged linearly and divided by the energy of the window to improve the consistency of the spectral estimates.

3.2.2 *Autocorrelation* The autocorrelation is important in that it reveals the presence of periodicity prevailing in the flow.

The equation in the discrete form is:

$$A_x(k\,\Delta t) = \frac{1}{M}\sum_{i=0}^{i=M-1} y(i\,\Delta t - k\,\Delta t)y(i\,\Delta t) \qquad (3)$$

Recognizing the fact that the autocorrelation and power spectral density functions are Fourier transform pairs, a novel method of deriving the autocorrelation was developed by Cooley *et al.* (**21**). This involves performing the inverse fast Fourier transform on the vector products which translates the Fourier coefficients from the frequency domain back into the time domain, thus reducing the computation time considerably. Using a generated sine wave, the autocorrelation routine gave a perfect sinusoid similar to the original. The coefficient $A_x(t)$ was normalized to unity for comparison.

3.2.3 *Measurement of* $u'/\bar{U}$ Two channels were used in conjunction with the sample and hold amplifiers on the ADC, permitting simultaneous recording of the fluctuations and the mean voltage. Subsequent linearization of the voltages on the computer was possible, since the hot wire probe had been calibrated over the flow range on a DISA 55D90 calibration apparatus, the ratio of $u'/\bar{U}$ being expressed as a percentage. Each value was recorded by taking the average of six data records, each of 15 s duration per channel. Measurements were made, at constant axial flow, with increasing inner cylinder speeds over the entire speed range. To check for consistency, these measurements were then repeated for decreasing speeds.

4 RESULTS AND DISCUSSION

4.1 Power spectrum and autocorrelation results

4.1.1 *Narrow gap case* ($N = 0{\cdot}955$) Figures 2 and 3 show the power spectra and auto-correlograms for increasing values of Ta/Ta_c at $Re_a = 500$. The use of a logarithmic scale for the power axes serves to emphasize any noise which may be present. Referring to Fig. 2(a), the onset of vortex flow is indicated by the single predominant frequency f_1 with its associated harmonics, occurring at $Ta_c = 19\,800$ corresponding to a speed of 7·5 rev/s. The frequency due to the axial flow component, although present, is difficult to discern and is

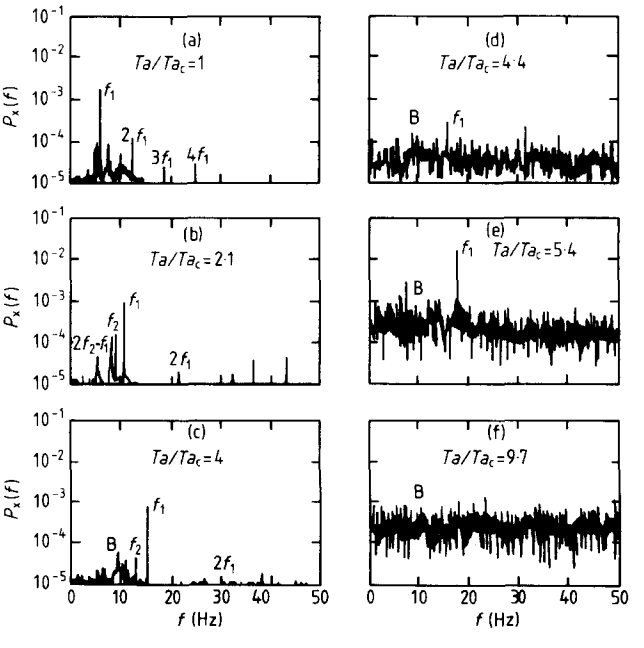

Fig. 2. Power spectra ($N = 0{\cdot}955$, $Re_a = 500$)

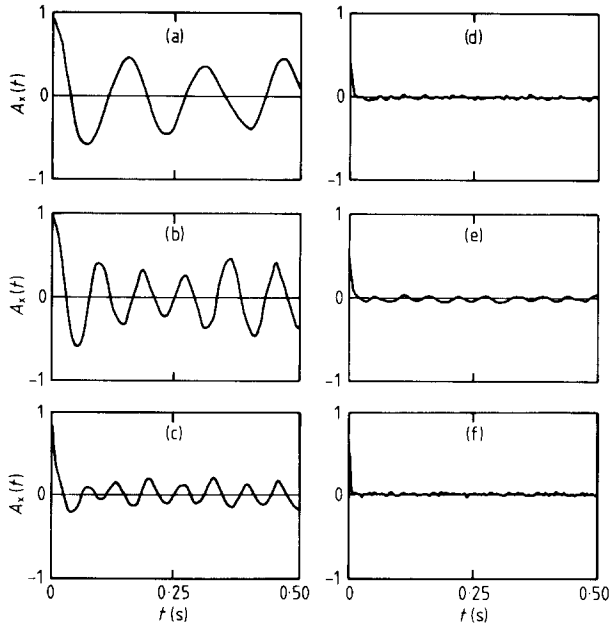

Fig. 3. Auto-correlograms ($N = 0{\cdot}955$, $Re_a = 500$). Note: Values of Ta/Ta_c correspond to those in Fig. 2.

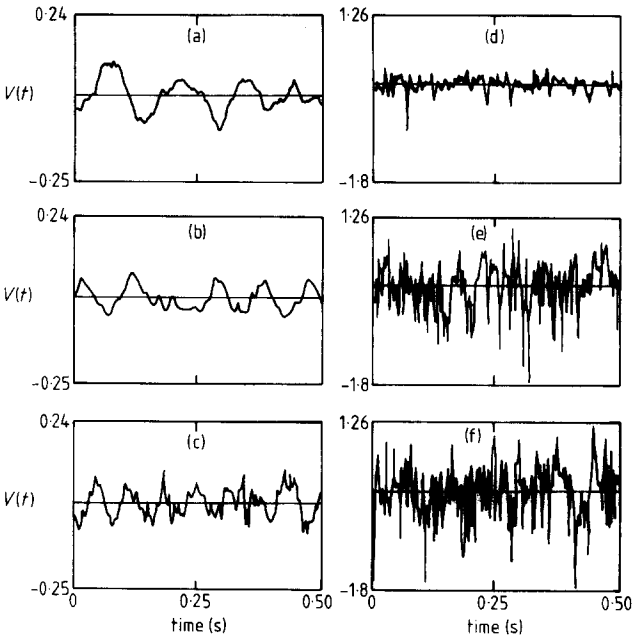

Fig. 4. Signal traces ($N = 0{\cdot}955$, $Re_a = 500$). Note: Values of Ta/Ta_c correspond to those in Fig. 2.

believed to be suppressed by the vortex motion. All higher transition modes correspond to harmonics of two fundamental frequencies of the vortex motion and the azimuthal mode. The appearance of a second frequency f_2 occurs at $Ta/Ta_c = 2{\cdot}1$ (Fig. 2(b)) together with a subharmonic of f_1 and f_2. At $Ta/Ta_c = 4$, (Fig. 2(c)) the spectrum increases in complexity as higher frequency modes of constant magnitude (commonly termed noise) appear in the background. The broadening of the sharp spectral lines is also observed indicating the breakdown of periodic flow. This broadband component B increases in power as well as in width as the Taylor number increases. It is interesting to note that Coles (**4**) described the flow in this state to be no longer laminar, in the sense that irregularities are beginning to appear, especially in the form of small scale motion. The transition into a quasiperiodic state with f_2 disappearing and f_1 superimposed in the chaotic band of frequencies occurs at $Ta/Ta_c = 4{\cdot}4$ (Fig. 2(d)), the presence of small scale eddies now being evident in the flow. The theorem of Newhouse *et al.* (**22**) concerning the nature of quasiperiodic flow states that two discrete frequencies characterize the flow in a transition to chaotic flow. From $Ta/Ta_c = 5{\cdot}4$ to $9{\cdot}7$, (Fig. 2(e) and (f)), the flow becomes weakly turbulent, a continuous spectrum developing.

The auto-correlograms (Fig. 3) correspond to the development of the flow illustrated in Fig. 2. Vortex flow and its higher modes are represented as a periodic trace. With the appearance of higher frequency components in the signal traces as shown in Fig. 4, the decay time becomes more rapid. With the first appearance and broadening of the spectral features, the auto-correlograms become non-periodic (Fig. 3(e) and (f)). At higher Taylor numbers, the significance of the function ceases as the chaotic mode ensues (Fig. 3(f)).

Higher axial flows, viz., $Re_a = 1500$ and 2500, were also studied. For comparison, the dominant spectral frequencies were normalized with respect to the inner cylinder frequency (f_c). Figure 5 is a plot of f/f_c vs Ta for $Re_a = 500$, 1500, and 2500. On this figure, a scale of Ta/Ta_c has been added but this is relevant only for $Re_a = 500$; it was found difficult accurately to determine the critical Taylor number at the two higher values of Re_a. The spectral frequency peak f_1 was present in all three cases and assumes a value very close to the inner cylinder frequency. Higher flows seem to have a suppressing influence on f_1. At $Re_a = 2500$, with the breakdown of laminar flow, an interesting phenomenon of reemergent flow is observed. The frequency peak f_1 appears and disappears for $16 \times 10^3 \leqslant Ta \leqslant 56 \times 10^3$ against a turbulent background. Also at

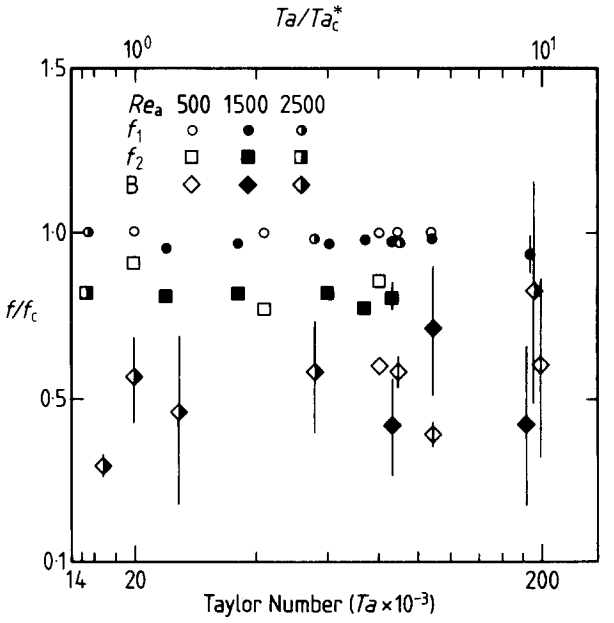

Fig. 5. Variation of f/f_c with Ta for $N = 0{\cdot}955$. *Relevant only to $Re_a = 500$

$Ta \approx 107 \times 10^3$, for all three values of Re_a, f_1 fades into the continuum.

The frequency peak f_2 occurs in all three axial flows, the higher flows tending to promote its appearance. These peaks are fairly close to the normalized frequency value of 0·8 and they exhibit a greater scatter than those for f_1.

The breakdown of flow from a quasiperiodic to a weakly turbulent mode (broadband component B) occurs at $Ta = 84{\cdot}7 \times 10^3$ for $Re_a = 1500$. Comparing this with $Ta = 79{\cdot}2 \times 10^3$ for $Re_a = 500$, the stabilizing effect of the axial flow is evident. For $Re_a = 2500$, however, the appearance of the spectral peaks occurs as early as $Ta \approx 14{\cdot}2 \times 10^3$. This breakdown was observed to be a gradual and repeatable process.

4.1.2 *Wide gap case* ($N = 0{\cdot}8$) The spectral evolution of the flow in the wide gap for $Re_a = 500$ is shown in Fig. 6. The spectra are very complicated and there are no sharply defined peaks as in the narrow gap case. Comparing the values of Ta_c for the wide gap with those for the narrow gap, it will be recognized that, for a given Re_a, a higher mean axial velocity prevails in the narrow gap, causing instability to occur at higher values of Ta. Consequently, for the inner cylinder speeds under investigation, the range of Ta/Ta_c will be considerably extended for the wide gap, to an order of 10^3, at which greater flow disturbances and broadening of the discrete frequencies occur. In Fig. 6(a) at $Ta/Ta_c = 1$, corresponding to a Taylor number of 10500 at a speed of 0·67 rev/s, a single peak is clearly discernible with noise starting to appear. A small increase in Ta/Ta_c led to this peak being lost in the complex spectrum (Fig. 6(b)). Further increase in Ta/Ta_c gave a continuous chaotic spectrum from which it is impossible to distinguish any broad spectral peaks or changes (Fig. 6(c) and (d)). This persists until $Ta/Ta_c = 506$ (Fig. 6(e)) when broad peaks begin to appear out of the chaos; this interesting phenomenon has been found to be repeatable. Even at $Ta/Ta_c = 1190$, (Fig. 6(f)) these spectral peaks are still

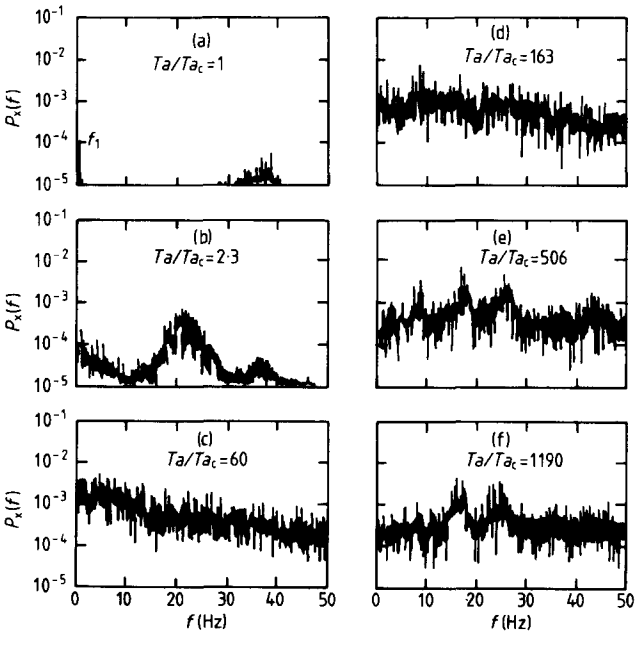

Fig. 6. Power spectra ($N = 0{\cdot}8$, $Re_a = 500$)

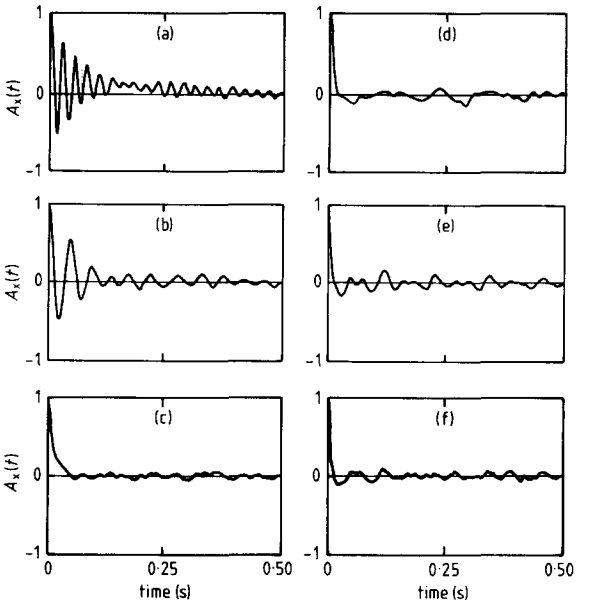

Fig. 7. Auto-correlograms ($N = 0{\cdot}8$, $Re_a = 500$). Note: Values of Ta/Ta_c correspond to those in Fig. 6

evident. Referring to the auto-correlograms for this flow (Fig. 7), the periodic nature for low values of Ta/Ta_c is seen in Fig. 7(a) and (b). Loss in correlation results when the flow becomes chaotic (Fig. 7(c) and (d)). The appearance of the broad spectral peaks is represented by the auto-correlogram reverting to a periodic form (Fig. 7(e)) having a crossover point similar to Fig. 7(b). At $Ta/Ta_c = 1190$ (Fig. 7(f)) the periodicity of the function is still persisting.

Other experiments were performed for higher flows, viz., $Re_a = 1500$ and 2500. The spectra for these conditions were generally very chaotic and attempts to present them in the form of Fig. 5 were unsuccessful due to their complexity. It was noted that the axial flow tends to delay the appearance of the broad spectral peaks. As was stated earlier, this occurs at $Ta = 5{\cdot}3 \times 10^6$ for $Re_a = 500$ (Fig. 6(e)). However, it is delayed until $7{\cdot}9 \times 10^6$ for $Re_a = 1500$ and does not appear at all in the present experimental range for $Re_a = 2500$.

4.2 Comparison with other Investigations

In their early work, Kaye and Elgar (**10**) detected the onset of turbulent plus vortex flow for $Re_a = 500$ at $Ta/Ta_c \approx 2$. It is interesting that this value corresponds to the appearance of the frequency peak f_2 in the present investigation (Fig. 2(b)). Using an apparatus of $N = 0{\cdot}727$, Astill (**13**) found that turbulence occurs later at $Ta/Ta_c = 4{\cdot}5$ for $Re_a = 500$. This is in good agreement with the present narrow gap results.

There is, however, a lack of information dealing with transition modes preceding turbulence. Notwithstanding this, extensive researches into this flow have been carried out recently for $Re_a = 0$ (**16, 23, 24**) with which the present results will now be compared. It should be appreciated that, because of the axial flow component, the values of the present Ta/Ta_c at which these transitions occur will be much lower than those for $Re_a = 0$.

Fenstermacher *et al.* (**16**) used digital techniques in their laser doppler measurement for $N = 0{\cdot}877$. They obtained similar transitions of flow to the present narrow gap results, their value of Ta_c being 1987. The appearance of f_2 was detected at $Ta/Ta_c = 228$, the flow becoming chaotic for $Ta/Ta_c \geqslant 529$. Although they detected a third frequency peak having a transient nature, this was not found in the present investigations. It is probable that it was suppressed as a result of the axial flow component. Cognet (**23**), using an ion technique to measure the flow, also found that two fundamental frequencies precede chaotic flow, disappearing at $Ta/Ta_c = 380$.

Walden and Donnelly (**24**) made visual observations and performed spectral studies from ion collector probes up to $Ta/Ta_c = 4489$ ($Ta_c = 1988$, $N = 0{\cdot}875$). They discovered that at $Ta/Ta_c \geqslant 784$, a definite peak re-emerged from the chaotic spectrum persisting to as high as $Ta/Ta_c = 1296$. They also found that, in some instances, the re-emergent peak was present throughout the entire Taylor number range but, at other times, it only occurred for part of the range. This regime was termed as one of 'latent order'. No conclusive evidence could be given as to why this phenomenon occurred, but since the apparatus used had a small length : gap ratio, it could have been due to end effects. This tendency seems to be evident in the present narrow gap results as the re-emergent peak can be seen for $Re_a = 2500$. These results add further insight into this phenomenon of re-emergence in that, with a high enough axial flow, this occurrence is displayed also. Current theories on transitions from laminar to turbulent flow reviewed by Martin (**25**) do not offer any clues as to why peak re-emergence occurs in a chaotic spectrum.

It is very probable that the phenomenon of the re-emerging broad spectral peaks observed in the wide gap is different from that of the re-emergent peaks observed in the narrow gap. One reason for this view is that the wide gap peaks have a distinctive broadband pattern with the spectral energies concentrated in the peaks unlike for the narrow gap. Also considering the Taylor number range, the values of Ta at which the broad peaks appear in the wide gap are far higher than those at which the distinct peaks are noted in the narrow gap.

Evidence supporting this onset of a periodic instability at high Taylor numbers for a wide gap can be found in the recent investigation of Koschmieder (**26**) for $Re_a = 0$, $N = 0{\cdot}72$. His results indicated that the supercritical Taylor vortex flow was well organized in the form of toroidal turbulent vortices of a uniform size. He found also that the wavelength of the turbulent vortices was substantially larger than the critical wavelength of laminar Taylor vortices. Barcilon *et al.* (**27**), studying the range $10^3 \leqslant Ta/Ta_c \leqslant 10^5$, reported a transition, at high Taylor numbers, from a complex pattern to a more ordered disturbance, having a low wave number persisting in the cell core. The visual observations of O'Brien (**28**) at $Ta \approx 108$ showed a basic vortex cell structure in the annulus with smaller spiral vortices on the outer wall, these latter being Görtler vortices co-existing at marginal stability with the basic vortex structure. Hence, it is suggested that broad spectral peaks of the present wide gap investigation are due to the formation of turbulent vortices in the annular gap. For low values of Re_a, the axial flow component is not significant compared with the high rotational component, thereby giving similar flow transitions to those observed at $Re_a = 0$.

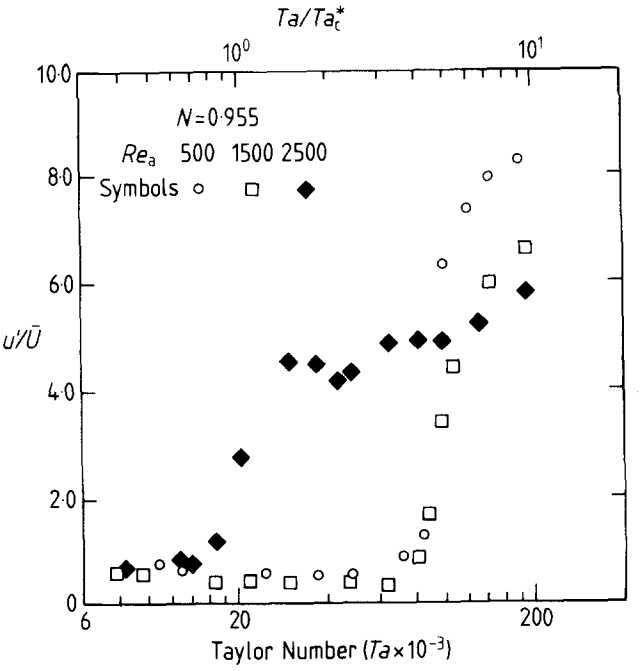

Fig. 8. Variation of $u'/\bar{U}$ with Ta for $N = 0{\cdot}955$. *Relevant only to $Re_a = 500$

A theoretical analysis of the turbulent plus Taylor vortex flow regime is of great difficulty due to the problem being nonlinear, which is further complicated if time dependent initial conditions are considered. The recent review by DiPrima (**29**) on nonlinear hydrodynamic stability analyses will perhaps direct more attention to this area.

4.3 Turbulence Intensity Results

Figure 8 shows results for the narrow gap investigation, the turbulence fluctuations being represented by $u'/\bar{U}$ where, at the mid gap position, u' is the r.m.s. velocity fluctuation and $\bar{U}$ the mean effective velocity of the flow (i.e., the vector sum of axial and rotational velocity components).

For $Re_a = 2500$, the increase in $u'/\bar{U}$ occurs earlier than for the lower values of Re_a, being attributed to the breakdown of the axial laminar flow. With the flow displaying the phenomenon of the re-emerging peaks, $55{\cdot}4 \times 10^3 \leqslant Ta \leqslant 89{\cdot}1 \times 10^3$, there is a decrease in the gradient to a constant level.

Figure 9 represents the results for the wide gap case. It will be noted that the Taylor number range has been extended and it might be argued that the results of Fig. 9 appear to be a progression of those of Fig. 8 into that range. For $Re_a = 500$, the initial steep gradient ($Ta/Ta_c < 2{\cdot}72$) is followed by a sharp drop after which the vigorous motion is shown to resume with a sharp increase at $Ta/Ta_c > 5{\cdot}6$. Then for $10{\cdot}6 \leqslant Ta/Ta_c \leqslant 289$, the values are virtually constant after which there is a decrease, corresponding to the appearance of the broad

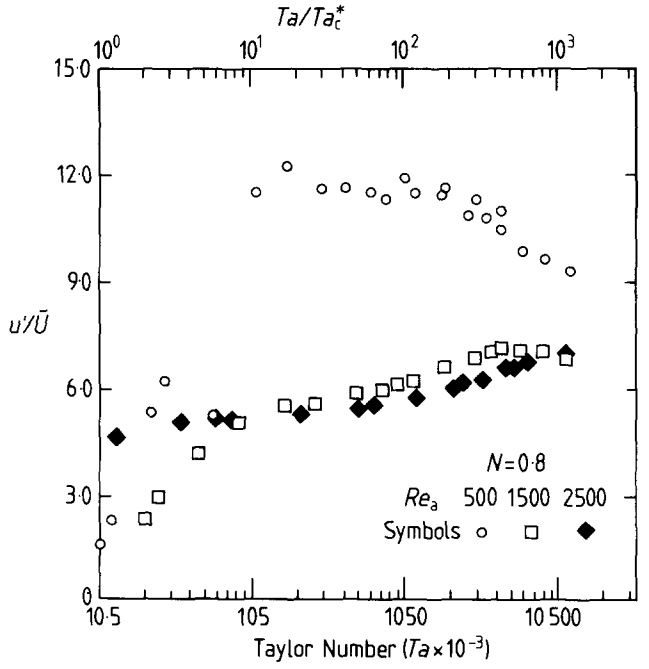

Fig. 9. Variation of $u'/\bar{U}$ with Ta for $N = 0{\cdot}8$. *Relevant only to $Re_a = 500$

spectral peaks (Fig. 6(e)). The spectra and auto-correlograms give no indication of these occurrences at $2{\cdot}7 \leqslant Ta/Ta_c \leqslant 5{\cdot}6$.

A slight decrease in $u'/\bar{U}$ is noticed at $Ta = 7{\cdot}9 \times 10^6$ for $Re_a = 1500$ also corresponding to the re-emergent broad peaks. For $Re_a = 2500$, where no such transition is seen to occur, there is no sign of any significant change in the intensity and it assumes a constant value of approximately $u'/\bar{U} = 5$.

Coney and Simmers (**30**) studied the variation of shear stress with Taylor number at the outer stationary surface of an annular gap of $N = 0{\cdot}833$ for $300 \leqslant Re_a \leqslant 1400$. For all values of Re_a, they found a sharp increase in shear stress at the critical Taylor number. However, for $Re_a = 300$ and 400, they also observed that at $Ta/Ta_c = 1{\cdot}8$ and $2{\cdot}4$ respectively, a further increase in the slope of the shear stress vs Ta plot occurred. Turning now to the present results for $Re_a = 500$, Fig. 9 shows that, at $Ta/Ta_c \approx 1{\cdot}8$, in the mid gap position, a sharp decrease of $u'/\bar{U}$ occurs with increase in Ta. Also, for $Re_a = 306$ and remembering that Fig. 9 pertains to $Re_a = 500$, this decrease occurs at $Ta/Ta_c \approx 3$ for a radial position 25 per cent of the gap width from the outer wall. It is suggested that these present phenomena and the subsequent flow developments are related to the observations of (**30**).

5 CONCLUSIONS

For both the wide and narrow gaps, a wide range of Ta/Ta_c was investigated. An accurate definition of the transitions to turbulent flow was achieved within a small range of Ta/Ta_c in the narrow gap. Here, the well defined fundamental frequencies were observed, indicating that the sequences of instabilities preceding turbulence need not necessarily be large, the transitional modes being in good agreement with recent investigations in Taylor vortex flow for $Re_a = 0$. The high axial flow does not seem to alter the occurrence of these transitions significantly in that the two peak frequencies are always discernible. Also, a gradual damping of the intensity of turbulence was observed with increasing axial flows.

There is evidence to suggest that the phenomena of re-emergence observed in the narrow and wide annular gaps are unique to each case: in the wide gap the reorientation of the flow to periodic turbulent vortices was observed. It is possible that nonlinear effects at finite amplitudes will cause energy transfer from the mean motion to the harmonics of the fundamental disturbance, as postulated by Stuart (**31**). However, the phenomenon of re-emergent peaks in the narrow gap for $Re_a = 2500$ has still to be explained.

REFERENCES

(1) TAYLOR, G. I. 'Stability of a Viscous Fluid Contained between Two Rotating Cylinders', *Phil. Trans. Roy. Soc.* 1923, **A223**, 289–343

(2) SNYDER, H. A. 'Experiments on the stability of spiral flow at low axial Reynolds numbers', *Proc. Roy. Soc.* 1965, **A265**, 198–214

(3) SCHWARZ, K. N., SPRINGETT, B. E., and DONNELLY, R. J. 'Modes of instability in spiral flow between rotating cylinders', *J. Fluid Mech.* 1964, **20**, 281–289

(4) COLES, D. 'Transition in Circular Couette Flow', *J. Fluid Mech.* 1965, **21**, 385–425

(5) CHANDRASEKAR, S. 'The hydrodynamic stability of viscid flow between coaxial cylinders', *Proc. Nat. Acad. Sc.* 1960, **46**, 141–143

(6) DiPRIMA, R. C. 'The Stability of Spiral Flow between Rotating Cylinders', *Proc. Roy. Soc.* 1962, **A265**, 188–197

(7) DATTA, S. K. 'Stability of Spiral Flow Between Concentric Rotating Cylinders at low axial Reynolds Numbers', *J. Fluid Mech.* 1965, **21**, 635–640

(8) DONNELLY, R. J. and FULTZ, D. 'Experiments on the Stability of Spiral Flow between Rotating Cylinders', *Proc. Nat. Acad. Sc.* 1960, **46**, 1150–1154

(9) HUGHES, T. H. and REID, W. H. 'The Stability of Spiral Flow between Rotating Cylinders', *Phil. Trans. Roy. Soc.* 1968, **263** (**A1135**), 57–91

(10) KAYE, J. and ELGAR, E. C. 'Modes of Adiabatic and Diabatic Fluid Flow in an Annulus with an Inner Rotating Cylinder', *Trans. ASME*, 1958, **80**, 753–765

(11) HASOON, M. A. and MARTIN, B. W. 'The Stability of Viscous Axial Flow in an Annulus with a Rotating Inner Cylinder', *Proc. Roy. Soc.* 1977, **A352**, 351–380

(12) GRAVAS, N. and MARTIN, B. W. 'Instability of Viscous Axial Flow in Annuli having a Rotating Inner Cylinder', *J. Fluid Mech.* 1978, **86** (Pt. 2), 385–394

(13) ASTILL, K. N. 'Studies in the Developing Flow Between Concentric Cylinders with the Inner Cylinder Rotating', *Trans. ASME* 1964, **C86** (3), 383–392

(14) GIBSON, C. H. 'Digital techniques in turbulence research', *AGARDograph* 1973, 174

(15) SWINNEY, H. L. and GOLLUB, J. P. 'The transition to turbulence', *Phys. Today* 1978, **31**, 41–49

(16) FENSTERMACHER, P. R., SWINNEY, H. L., and GOLLUB, J. P. 'Dynamical Instabilities and the Transition to Chaotic Taylor Vortex Flow', *J. Fluid Mech.* 1979, **94** (Pt. 1), 103

(17) SIMMERS, D. A. and CONEY, J. E. R. 'A Reynolds analogy solution for the heat transfer characteristics of combined Taylor vortex and axial flows', *Int. J. Heat Mass Transfer* 1979, **22**, 679–689

(18) SIMMERS, D. A. and CONEY, J. E. R. 'The effect of Taylor vortex flow on the development length in concentric annuli', *J. Mech. Engng. Sci.* 1979, **21** (2), 59–64

(19) OTNES, R. K. and ENOCHSON, L. *Digital Time Series Analysis* 1972, (Wiley, New York)

(20) HANCOCK, J. C. *An Introduction to the Principles of Communication Theory*, 1961 (McGraw-Hill, New York, Toronto, London)

(21) COOLEY, J. W., LEWIS, P. A. W., and WELCH, P. D., 'The Fast Fourier Transform and its Application', *IEEE Trans. on Education* 1969, **12** (No. 1), 27134

(22) NEWHOUSE, S., RUELLE, D., and TAKENS, F. 'Occurrence of strange Axiom A attractors near quasiperiodic flows on T^m, $m \geqslant 3$', *Commun. Math. Phys.* 1978, **64**, 35–40
(23) COGNET, G. J. 'Transition to Taylor Couette Flow in a small gap configuration', *Taylor Vortex Flow Working Party Meeting*, Mech. Eng. Dept., University of Leeds, 1979, 15–20
(24) WALDEN, R. W. and DONNELLY, R. J. 'Re-emergent Order of Chaotic Circular Couette Flow,' *Phys. Rev. Lett.* 1979, **42**, 301–304
(25) MARTIN, P. C. *Proceedings of the International Conference on Statistical Physics, Budapest* 1975, edited by L. Pal and P. Szepfalusy
(26) KOSCHMIEDER, E. L. 'Turbulent Taylor Vortex Flow', *J. Fluid Mech.* 1979, **93** (Pt. 3), 515–527
(27) BARCILON, A., BRINDLEY, J., LESSEN, M., and MOBBS, F. R. 'Marginal instability in Taylor–Couette flows at a very high Taylor number', *J. Fluid Mech.* 1979, **94** (Pt. 3), 453–463
(28) O'BRIEN, K. T. *Evaluation of turbulence between eccentric rotating cylinders* 1974, PhD Thesis, Leeds
(29) DiPRIMA, R. C. *Eighth U.S. Nat. Congr. Appl. Mech.*, UCLA, 1978
(30) CONEY, J. E. R. and SIMMERS, D. A. 'A study of fully-developed, laminar, axial flow and Taylor vortex flow by means of shear stress measurements', *J. Mech. Engng. Sci.* 1979, **21** (No. 1), 19–24
(31) STUART, J. T., 'On the nonlinear mechanics of hydrodynamic stability', *J. Fluid Mech.* 1958, **4**, 1–21